In vivo fluid dynamics of the Ventura interatrial shunt device in patients with heart failure

Pfeiffer, M.; Boehmer, J.; Gorcsan, J.; Eguchi, S.; Orihara, Y.; Perl, M.L.; ... ; Bax, J.J.

ESC HEART FAILURE
ESC Heart Failure 2024; **11**: 2499–2509
Published online 22 May 2024 in Wiley Online Library (wileyonlinelibrary.com) **DOI:** 10.1002/ehf2.14859

ORIGINAL ARTICLE

In vivo fluid dynamics of the Ventura interatrial shunt device in patients with heart failure

Michael Pfeiffer[1]*, John Boehmer[1], John Gorcsan[1], Shunsuke Eguchi[1], Yoshiyuki Orihara[1], Michal Laufer Perl[2], Neal Eigler[3], William T. Abraham[4], Julio Nuñez Villota[5], Elizabeth Lee[6], Antoni Bayés-Genís[7], Gil Moravsky[8], Saibal Kar[9], Michael R. Zile[10], Richard Holcomb[11], Stefan D. Anker[12], Gregg W. Stone[13], Josep Rodés-Cabau[14], JoAnn Lindenfeld[15] and Jeroen J. Bax[16]

[1]*Division of Cardiology, Penn State Heart and Vascular Institute, Milton S. Hershey Medical Center, Hershey, Pennsylvania, USA;* [2]*Division of Cardiology, Sammy Ofer Heart Center, Tel Aviv Sourasky Medical Center, Tel Aviv-Yafo, Israel;* [3]*V-Wave, Agoura Hills, California, and Department of Cardiology, Smidt Heart Institute, Cedars Sinai Medical Center, Los Angeles, California, USA;* [4]*Division of Cardiovascular Medicine, Davis Heart and Lung Research Institute, The Ohio State University Wexner Medical Center, Columbus, Ohio, USA;* [5]*Department of Cardiology, University of Valencia, Valencia, Spain;* [6]*Division of Cardiology, Rochester General Hospital, Rochester, New York, USA;* [7]*Department of Cardiology, Germans Trias Heart Institute, Germans Trias University Hospital, Badalona, Spain;* [8]*Division of Cardiology, Shamir Medical Center (Assaf HaRofeh), Be'er Ya'akov, Israel;* [9]*Cardiovascular Institute of Los Robles Health System, Los Robles, California, USA;* [10]*Division of Cardiology, Medical University of South Carolina, Ralph H. Johnson Department of Veterans Affairs Medical Center, Charleston, South Carolina, USA;* [11]*Independent Biostatistician, Minneapolis, Minnesota, USA;* [12]*Department of Cardiology (CVK) of German Heart Center Charité, Institute of Health Center for Regenerative Therapies (BCRT), German Centre for Cardiovascular Research (DZHK) partner site Berlin, Charité University, Berlin, Germany;* [13]*The Zena and Michael A. Wiener Cardiovascular Institute, Icahn School of Medicine at Mount Sinai, New York, USA;* [14]*Quebec Heart & Lung Institute, Laval University, Quebec City, Canada;* [15]*Division of Cardiology, Vanderbilt University Medical Center, Nashville, Tennessee, USA; and* [16]*Department of Cardiology, Leiden University Medical Center, Leiden, The Netherlands*

Abstract

Aims Interatrial shunts are under evaluation as a treatment for heart failure (HF); however, their *in vivo* flow performance has not been quantitatively studied. We aimed to investigate the fluid dynamics properties of the 0.51 cm orifice diameter Ventura shunt and assess its lumen integrity with serial transesophageal echocardiography (TEE).

Methods and results Computational fluid dynamics (CFD) and bench flow tests were used to establish the flow-pressure relationship of the shunt. Open-label patients from the RELIEVE-HF trial underwent TEE at shunt implant and at 6 and 12 month follow-up. Shunt effective diameter (D_{eff}) was derived from the *vena contracta*, and flow was determined by the continuity equation. CFD and bench studies independently validated that the shunt's discharge coefficient was 0.88 to 0.89. The device was successfully implanted in all 97 enrolled patients; mean age was 70 ± 11 years, 97% were NYHA class III, and 51% had LVEF ≤40%. Patency was confirmed in all instances, except for one stenotic shunt at 6 months. D_{eff} remained unchanged from baseline at 12 months (0.47 ± 0.01 cm, P = 0.376), as did the trans-shunt mean pressure gradient (5.1 ± 3.9 mmHg, P = 0.316) and flow (1137 ± 463 mL/min, P = 0.384). TEE measured flow versus pressure closely correlated ($R^2 \geq 0.98$) with a fluid dynamics model. At 12 months, the pulmonary/systemic flow Qp/Qs ratio was 1.22 ± 0.12.

Conclusions When implanted in patients with advanced HF, this small interatrial shunt demonstrated predictable and durable patency and performance.

Keywords Flow dynamics; Heart failure; Interatrial shunt; Transesophageal echocardiography

Received: 12 February 2024; Revised: 25 March 2024; Accepted: 24 April 2024
**Correspondence to: Michael Pfeiffer, Division of Cardiology, Penn State Heart and Vascular Institute, Milton S. Hershey Medical Center, Penn State College of Medicine, 500 University Dr, Hershey, PA 17033, USA. Email: mpfeiffer@pennstatehealth.psu.edu*
Clinical Trial Registration: ClinicalTrials.gov NCT03499236.

Introduction

Interatrial shunt devices and catheters that create iatrogenic atrial septal defects (iASD) to decompress the left atrium in patients with heart failure (HF) are under investigation.[1–7] Although most of these approaches create a shunt with orifice diameters that range from 0.6 to 1.0 cm, the actual orifice dimensions may vary depending on distortion caused by the topography of the interatrial septum or interventional placement methods. As such, it may be difficult to *a*

priori model how well a device or iASD will transmit flow *in vivo*. Moreover, as tissue injured during shunt creation heals, pannus formation may narrow the shunt lumen. Thus far, human studies have mostly taken a non-quantitative or binary approach, with patency defined by the presence of trans-shunt flow by transthoracic echocardiography (TTE).

The Ventura® Interatrial Shunt (V-Wave Ltd., Caesarea, IL), with its encapsulated hourglass shape and small 0.51 cm orifice, was designed so that variations in septal anatomy and/or healing would be less likely to affect shunt lumen dimensions. The objectives of this report were: first, to establish the properties of this shunt by computational fluid dynamics (CFD) simulations and bench flow tests, with comparison with standard haemodynamic equations; and second, to use serial transesophageal or intra-cardiac echocardiographic examinations (TEE or ICE) in HF patients to quantify shunt lumen dimensions and pressure versus flow relationships at device implantation through 12 months of follow-up.

Methods

Study device

The Ventura Interatrial Shunt, shown in *Figure 1A*, is built on an hourglass-shaped self-expanding nitinol frame that is encapsulated with sintered expanded polytetrafluoroethylene (ePTFE) on both its luminal and external (abluminal) surfaces. The encapsulant has an internodal distance of $\leq$30 μ. The shunt has a length of 1.2 cm, with a left atrial entry diameter of 1.4 cm, a right atrial exit diameter of 1.1 cm, and a wall thickness of 0.02 cm. The neck internal diameter is 0.51 cm with a manufacturing tolerance of ±0.01 cm. After transseptal catheterization, a custom delivery catheter is used to place the shunt so that its lumen spans the interatrial septum, which may not exceed 0.6 cm in thickness.

Computational fluid dynamics simulations

CFD simulations were conducted to analyse the shunt's velocity and pressure profiles, wall shear stress, and turbulence effects. Steady-state, left-to-right atrial pressure gradients of 6, 10, 14, and 30 mmHg were used for the simulations. The analyses were performed using a finite volume method software based on the Navier–Stokes equations (3DEXPERIENCE Fluid Dynamics Engineer, Dassault Systèmes, Paris, FR). The simulations were created from computer-aided design files, focusing on a 30-degree sector around the shunt's axis of symmetry. The meshed model consisted of approximately 350 K predominantly hexahedral elements. The fluid was modelled as Newtonian, with blood density set at 1.050 g/mL and a dynamic viscosity of 0.0035 Pa·s. Blood element exposure times were estimated for half-maximum or greater wall shear stress, and maximal vorticity was expressed as the curl of velocity vector.

Bench flow testing

Flow rates across the shunt were measured in a custom-made flow test apparatus (BDC Laboratories model FL68, Wheat Ridge, Colorado, USA) using saline at 37 ± 2°C with a density of 1.005 g/mL. The apparatus mimicked the left and right atria and their respective circulatory loops. Flowmeters and pressure sensors monitored inflow and outflow from each atrium. Twenty shunts certified for clinical use from six manufacturing lots were tested. Each shunt underwent evaluation at pressure gradients ranging from 2 to 20 mmHg with 2 mmHg increments.

In vivo evaluation

The REducing Lung congestIon symptoms using the v-wavE shunt in adVancEd Heart Failure (RELIEVE-HF) trial (NCT03499236)[8] is a multicentre pivotal study being performed under an FDA Investigational Device Exemption in HF patients who are NYHA functional class II–IV, regardless of LVEF. The protocol was approved by the IRB/Ethics Committee at all investigational sites, and all patients signed informed consent. This report focuses on the open-label, roll-in arm comprising 97 patients. Patients received dual antiplatelet agents for 6 months or continued oral anticoagulants if there were other pre-existing indications. Roll-in patients underwent TEE (N = 89) or ICE (N = 8) imaging during device implantation. Follow-up TEE/TTE exams were performed at 6 and 12 months.[9] TTE data other than for shunt patency and pulmonic to aortic flow ratios (Qp:Qs) have been reported elsewhere. Simultaneously, RELIEVE-HF enrolled a randomized, double-masked, sham-controlled cohort of 508 patients with the same entry criteria who are still undergoing clinical follow-up.

Analytical and statistical methods

CFD, bench flow, and *in vivo* measurements of shunt flow and pressure gradients were compared with the haemodynamic equations developed by Gorlin and Gorlin[10] as later modified by Flachskampf et al.,[11] for effective orifice size. Briefly, the flow through a restrictive orifice was modelled by combining the continuity and simplified Bernoulli equations such that

Figure 1 Shunt device and computational flow dynamics (CFD) examples. (A) Anterior perspective rendering of study device showing the ePTFE encapsulated shunt. (B–E) CFD half shunt sections spatial distribution of gauge pressure, velocity, wall shear stress and vorticity during steady state flow at pressure differential of 10 mmHg.

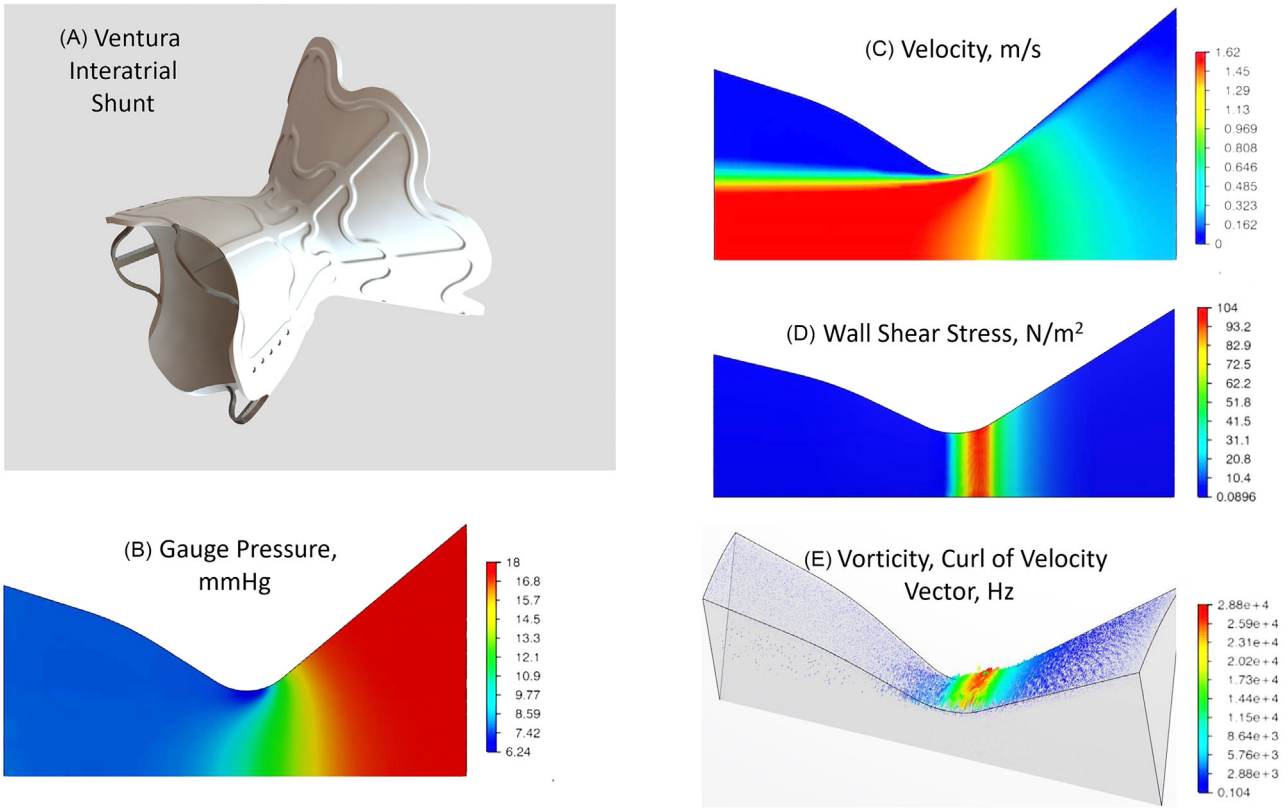

$$Q = 60 \times A_{orifice} c_D \left(\frac{2K\Delta\bar{P}}{\rho}\right)^{0.5} \quad (1)$$

where Q is flow in mL/min, $A_{orifice}$ is the true orifice area in cm^2, c_D is the discharge coefficient, K is the conversion 1 mmHg = 1333 dyne/cm^2, $\Delta\bar{P}$ is the mean pressure gradient in mmHg, ρ is fluid density in g/mL, and 60 converts seconds into minutes. c_D is a dimensionless parameter that relates viscous loss of velocity between the true orifice and the *vena contracta*. Values for c_D of the shunt were independently derived from the CFD and bench flow data.

The effective orifice area is therefore

$$A_{eff} = A_{orifice} c_D \quad (2)$$

Combining the above equations further reduces the flow model to

$$Q = 3024 \times A_{eff} \Delta\bar{P}^{0.5} \quad (3)$$

The constant 3024 differs from Flachskampf's[11] constant of 50.4, so that Q has a time base in minutes rather than seconds.

Echocardiographic studies were standardized in accordance with the echocardiographic manual specified by the centralized core laboratory (Penn State College of Medicine, Hershey, PA, USA). Two-dimensional TEE/ICE colour and continuous wave Doppler images of shunt flow were acquired over at least three cardiac cycles × 2 in multiple views optimized so that the ultrasonic beam was substantially coplanar with the central axis of the shunt lumen. Studies were read by the core lab without reference to prior or later studies. Shunt patency was defined if Doppler flow through the shunt lumen was seen on any TEE or TTE study from the specified time point or if no study was available, from a later follow-up study echocardiogram. For quantitation of pressure gradient, *vena contracta*, and shunt flow, only TEE or ICE studies from the specified time point were used. Multiple frames were assessed to visualize flow through the length of the shunt. The location for measuring the *vena contracta* diameter (D_{vc}) was confined within the shunt frame outline.

There may be errors in determining D_{vc} due to non-coaxial alignment of the echo beam with the shunt such that measurements are artefactually too small (pseudo-stenosis).

To correct for these distortions, the effective shunt diameter (D_{eff}) was calculated as

$$D_{eff} = D_{vc} \times \frac{D_{frame\ \ true}}{D_{frame\ \ measured}} \quad (4)$$

This equation uses the known inner diameter of the frame neck (0.52 cm) for calibration. $D_{frame\ measured}$ was assessed from the same echo image as D_{vc}. When the frame could not be measured (N = 6, 2.8%), D_{eff} was assigned the value of D_{vc}. Interobserver reliability for D_{vc} and D_{eff} was validated by the core laboratory. Shunts were empirically categorized as stenotic if D_{eff} were ≤0.38 cm, representing a 0.10 cm diameter lumen loss or ≥35% reduction in cross-sectional area. If $D_{vc} \leq 0.38$ cm, but D_{eff} was >0.38 cm, shunts were deemed pseudo-stenotic. TEE derived Q was evaluated by the continuity equation using separate A_{vc} and A_{eff} assessments of cross-sectional orifice area. Qp:Qs was calculated by both the standard TTE continuity equation method and by using TEE measured shunt flow plus aortic flow to estimate Qp.

Data in text and tables are mean ± standard deviation or median [interquartile range], unless otherwise stated. Comparisons of data from serial time points were by one-way repeated measures ANOVA, with sensitivity analysis for missing data by nearest neighbour. Comparisons of paired variances was by Levene's test. The goodness-of-fit to mathematical models were assessed by R^2, which were compared using Fisher's z-transformation.

Results

Simulations and bench studies

CFD simulations yielded a c_D averaging 0.884 ± 0.008. The effective area and diameter were 0.179 cm2 and 0.478 cm respectively at a pressure drop of 10 mmHg. These values were stable over the tested gradients. *Figure 1B–E* illustrates the spatial distributions of velocity, pressure, shear wall stress, and vorticity within the shunt lumen. The regions of highest wall shear stress and vorticity were confined to a region of ~0.11 cm axial length of the shunt, just proximal to and involving the central orifice.

Figure 2 depicts the relationship between Q and $\Delta\bar{P}$ obtained from CFD simulations in blood and bench flow measurements in saline. The bench measurements were reproducible, with standard deviations averaging 2.9% of the total flow. The measured c_D from the bench experiments was 0.875 ± 0.006. Both datasets were well described by the flow model equation (1), which only differed in the values for c_D and fluid density of saline or blood ($R^2 > 0.99$ for each model fit).

Figure 2 Computational flow dynamics (CFD) and *in vitro* bench measurement of shunt device flow/pressure relationship. ● represents data from CFD simulations in blood and ▲ are bench measurements in saline. Error bars are standard deviations. Curved lines are respective fits to model haemodynamic equation (1) with $R^2 > 0.99$ for each fit. ΔP^-, mean pressure gradient; Q, flow.

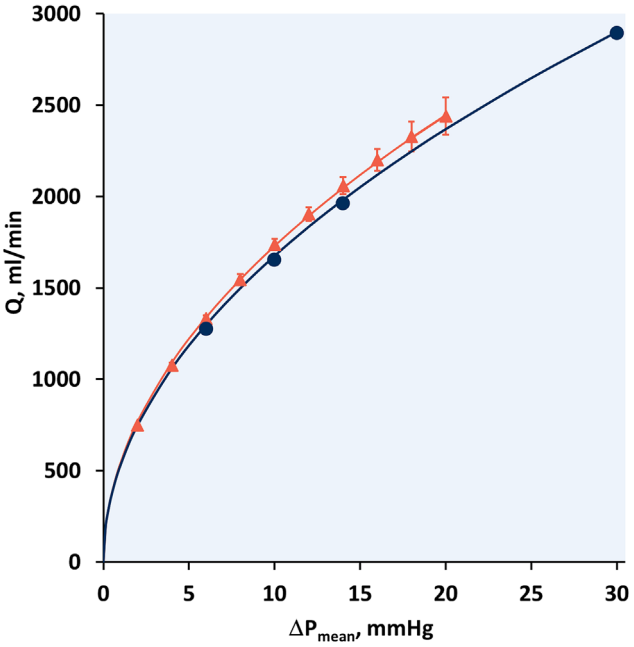

Clinical imaging evaluations

The RELIEVE-HF Roll-in cohort consisted of 97 patients enrolled at 64 sites across multiple countries, including the US, Israel, Spain, Germany, Poland, The Netherlands, Belgium, Switzerland, and Australia. The first patient was implanted on 9 September 2018, and the last 12 month follow-up was completed on 8 September 2022. Baseline patient characteristics are detailed in *Table 1*. The patients were elderly with predominantly NYHA Class III HF, a history of frequent prior HF hospitalizations, and a high incidence of co-morbidities including atrial fibrillation, hypertension, diabetes, and chronic kidney disease. They remained symptomatic despite treatment with maximally tolerated guideline-directed medical and device therapies, as confirmed by an Eligibility Committee. LV function was evenly divided between preserved and reduced LVEF with a cut-off for preserved LVEF at >40%, and they had mildly reduced right ventricular systolic function and abnormal resting haemodynamics with elevated filling pressures, reduced cardiac index, and elevated pulmonary vascular resistance. The population was high risk with a median NT-proBNP of 1730 pg/mL and MAGGIC[12] and BCN BIO-HF[13] expected 1-year mortality rates exceeding 20%. All patients were successfully implanted with the shunt.

Table 1 Baseline patient characteristics (n = 97)

Demographics	
Age, years	70 ± 11
Female	28 (28.9%)
BMI, kg/m^2	31.6 ± 5.6
Duration of HF, years	5.5 ± 5.0
HF hospitalizations per patient in prior year	1.0 ± 1.2
Co-morbidities	
Ischaemic aetiology	54 (55.7%)
Atrial fibrillation	50 (51.5%)
Hypertension	83 (85.6%)
Diabetes	53 (54.6%)
CKD	75 (80.4%)
COPD	26 (26.8%)
Stroke	17 (17.5%)
Therapies	
ICD/CRT	23 (23.7%)
CRT	24 (24.7%)
RASI	74 (76.3%)
Beta-blocker	82 (84.5%)
MRA	58 (59.8%)
SGLT2i	15 (15.5%)
Loop diuretics	92 (94.8%)
Measurements	
Hgb, g/dL	12.9 ± 1.9
eGFR, mL/min/1.73 m^2 (median [IQR])	42 [34–55]
LVEF, %	43 ± 16
RVFAC, %	36 ± 6
TAPSE, mm	16 ± 3
HR, b.p.m.	72 ± 12
BP systolic, mmHg	121 ± 17
RAP, mmHg	11 ± 5
PCWP, mmHg	20 ± 7
LA-RA gradient, mmHg	8 ± 5
PAP mean, mmHg	30 ± 8
CI, L/min/m^2	2.3 ± 0.8
PVR, Wood units	2.5 ± 1.2
Prognosis	
NYHA class III	94 (96.9%)
NYHA class IV	3 (3.1%)
KCCQ overall score	46 ± 21
6MWD, m	266 ± 89
NT-proBNP, pg/mL (median [IQR])	1730 [1076–3518]
BNP, pg/mL (median [IQR])	280 [151–769]
MAGGIC 1 year mortality, %	21 ± 11
BCN BIO-HF 1 year mortality, %	22 ± 15

Data expressed as number (%), mean ± standard deviation, or median [interquartile range].
6MWT, 6 minute walk test; BCN BIO-HF, Barcelona Bio-HF risk calculator; BMI, body mass index; BNP, brain natriuretic peptide; BP, blood pressure; CI, cardiac index; CKD, chronic kidney disease; COPD, chronic obstructive pulmonary disease; CRT, cardiac resynchronization therapy; eGFR, estimated glomerular filtration rate; HF Hosp, heart failure hospitalization; HF, heart rate; HFpEF, HF with preserved EF; HFrEF, HF with reduced ejection fraction (EF); Hgb, haemoglobin; ICD, implantable cardioverter defibrillator; KCCQ, Kansas City Cardiomyopathy Questionnaire; LA, left atrium; LVEF, left ventricular EF; MAGGIC, The Meta-Analysis Global Group in Chronic HF risk calculator; MI, myocardial infarction; MRA, mineralocorticoid receptor antagonist; NT-proBNP, N-terminal pro-brain natriuretic peptide; NYHA, New York Heart Association; PAP, pulmonary artery pressure; PCWP, pulmonary capillary wedge pressure; PVR, pulmonary vascular resistance; RA, right atrium; RAP, right atrial pressure; RASI, renin angiotensin system inhibitor; RVFAC, right ventricular fractional area change; SGLT2i, sodium glucose cotransporter 2 inhibitors; TAPSE, tricuspid annular plane systolic excursion.

Table 2 summarizes the echocardiographic assessments of shunt function at implant and at 6 and 12 month follow-up. The number of observations decreased over time, with 75 exams at 12 months [22 patients could not be assessed: 13 due to death, 1 due to left ventricular assist device (LVAD) placement, 1 patient withdrew from the study, and 7 missed clinic visits due to COVID-19 or related reasons]. All evaluable studies revealed patent shunts with continuous left-to-right flow in 244 out of 256 examinations (95.3%), while the remainder exhibited bidirectional flow. Bidirectional flow tended to be intermittent, varying with respiration and associated with a low $\Delta\bar{P}$ (1.5 ± 1.4 mmHg). The measurements of D_{vc} and D_{eff} averaged 0.45 and 0.47 cm, respectively, and remained stable over time. For all patients and time points, $\Delta\bar{P}$ averaged from 4 to 5 mmHg, and the flow rate (Q) averaged 1037 to 1137 mL/min without statistically significant changes over the duration of follow-up.

Figure 3 (Central Illustration) shows representative TEE colour and continuous wave Doppler images from a patient with a widely patent shunt with nominal values for D_{vc}, $D_{frame\ measured}$, and D_{eff} at 12 month follow-up. *Figure 4* illustrates colour Doppler images of stenotic and pseudo-stenotic shunts and their associated measurements.

Figure 5 plots individual patient measurements of D_{vc}, $D_{frame\ measured}$, and D_{eff} at implant, and at 6 and 12 month follow-up. Applying $D_{frame\ measured}$ as a correction for non-coaxial imaging to estimate D_{eff} per equation (4) significantly reduced the observed variances ($P < 0.001$) at implant when stenotic shunts were not possible, and also at 6 and 12 month follow-up. A single patient had a stenotic shunt at 6 month follow-up, which was placed in the anterior/superior part of the interventricular septum, consistent with the location of a foramen ovale track (*Figure 4*). The length of the shunt confined within the septum exceeded the shunt's design limits at 0.9 cm, and the right atrial side of the shunt remained intra-septal. Although there was initial clinical improvement, the patient's condition deteriorated, requiring left ventricular assist device (LVAD) placement after 8 months, during which the surgeon reported shunt occlusion.

There were 19 instances of pseudo-stenosis in 18 patients (9 at implant, 6 at 6 month, and 4 at 12 month follow-up). In 11 instances, the patient had a later follow-up TEE with a normal D_{vc} measurement. One patient had pseudo-stenosis at both 6 and 12 months; D_{vc} measured 0.35 cm both times while D_{eff} remained nominal at 0.49 and 0.47 cm, respectively.

At 12 months, D_{eff} could not be evaluated in 30 of 82 (37%) patients remaining in the study, but all 30 had a TEE at 6 months, during which D_{eff} was unnarrowed at 0.48 ± 0.01 cm. In these cases, the septal thickness adjacent to the shunt was within design limits averaging 0.23 ± 0.08 cm, and in all cases, the right atrial cone of the shunt frame extended into the right atrium.

Table 2 Echocardiographic assessments of shunt function

	Implant	6 months	12 months	*P*-value
Eligible patients				
N	97	90	82	
Studies analysed				
TEE or TTE	97 (100%)	87 (97%)	75 (91%)	
TEE	86 (89%)	69 (77%)	56 (68%)	
Time to TEE, months	0 [0–0]	6.2 [5.7–6.6]	12.3 [11.9–12.9]	
Results				
Shunt patent	97 (100%)	87 (100%)	72 (100%)[a]	1.000
Flow direction				
Left to right	91 (94%)	85 (98%)	68 (94%)	0.895
Right to left	0 (0%)	0 (0%)	0 (0%)	
Bidirectional	6 (6%)	2 (2%)	4 (6%)	
Shunt thrombi	0	0	0[b]	
D_{vc}, mm	4.5 ± 0.5	4.5 ± 0.6	4.5 ± 0.4	0.092
D_{eff}, mm	4.7 ± 0.1	4.7 ± 0.4	4.7 ± 0.1	0.376
C_d	0.87 ± 0.05	0.86 ± 0.10	0.86 ± 0.04	0.363
$\Delta\bar{P}$, mmHg	4.2 ± 2.9	5.1 ± 3.1	5.1 ± 3.9	0.316
Q, mL/min	1037 ± 385	1124 ± 417	1137 ± 463	0.384

Data expressed as *N* (% eligible patients), median [IQR], or mean ± SD and are inclusive of a single stenotic shunt at 6 months.

$\Delta\bar{P}$ = mean interatrial pressure gradient; C_d = discharge coefficient; D_{eff} = effective diameter; D_{vc} = *vena contracta* diameter; Q = flow.
[a]Three cases with echocardiographic imaging, but no colour Doppler views of the shunt.
[b]Thrombus seen in left atrial appendage in one patient.

Figure 6 shows TEE measured Q as a function of $\Delta\bar{P}$ at each time point. The correlation with CFD model estimates of Q was improved when TEE measurements used A_{eff} compared with A_{vc} to compute flow (R^2: 0.98 vs. 0.80, $P < 0.001$). Qp: Qs at 12 month follow-up was 1.22 ± 0.12 using TEE measured shunt flow compared with 1.24 ± 0.40 by TTE continuity equation. Although these methods yielded similar averages ($P = 0.663$), the TEE shunt flow method had improved variance ($P < 0.001$).

Discussion

The present study is the first comprehensive characterization of the theoretical and *in vivo* performance of the Ventura® Interatrial Shunt device using a combination of CFD simulations, bench flow measurements, and invasive echocardiography in patients with advanced HF. The results from CFD and bench flow studies were consistent with previously validated haemodynamic models. Serial TEE examinations at the time of shunt implantation and at 6 month and 12 month follow-up provided insights into the shunt's performance under physiological conditions and demonstrated the durability of the shunt size with minimal late lumen loss observed during the expected healing period.

Theoretical background

CFD simulations are powerful tools for designing and verifying implantable cardiovascular devices.[14] The slight differences in shunt flow between blood and saline observed in the respective simulations and bench measurements can be attributed to blood's higher density and viscosity. The coefficients of discharge c_D obtained from CFD and bench measurements were in good agreement, each averaging 0.88, and were slightly less than the published range (0.91–0.94) for smoothed walled convergent/divergent Venturi nozzles at the Reynolds numbers expected during physiological shunting.[15] This is likely the result of the shunt's more rapid pre-orifice taper and the rougher surface of the ePTFE encapsulant. Despite this, the shunt demonstrated less viscous losses compared with congenital secundum atrial septal defects, which have modelled c_D values closer to those of CFD modelled classical fluid mechanics flat plate orifices, which ranges from 0.62 to 0.71.[15] Flachskampf et al.[12] reported a c_D of 0.72 in bench flow measurements of a flat plate orifice with diameter 0.6 cm under physiological pressure and flow conditions similar to the present bench studies.

Results for wall shear stress, exposure time, and turbulent flow including Reynolds numbers and vorticity were consistent with prior studies that correlated with a low likelihood for haemolysis or platelet activation.[16–19] Also, these parameters were less severe than observed in the normal aorta, or with pathological conditions such as mitral paravalvular leaks, aortic stenosis, or with implanted prostheses including LVADs.[20–22] As there are no accepted criteria, adverse event data from randomized controlled trials may best inform whether there are any rheological concerns with this shunt device.

In vivo shunt performance

At implant, TEE measurements of the *vena contracta* averaged 0.45 ± 0.05 cm, which is lower than the effective

Figure 3 Central illustration: Transesophageal echocardiographic (TEE) images of a widely patent shunt. Images from 12 month follow-up in a 67-year-old male with non-ischaemic cardiomyopathy. Top: Colour Doppler short axis view showing shunt frame and locations of the *vena contracta* and frame neck diameter measurements. Mid: Continuous wave Doppler through the shunt with dotted line indicating mean velocity. Bottom: Measured fluid dynamics values. ΔP^{-}, mean interatrial pressure gradient; D_{eff}, effective diameter; D_{frame}, measured diameter of the frame neck; D_{vc}, diameter *vena contracta*; LA, left atrium; Q, trans-shunt flow; RA, right atrium.

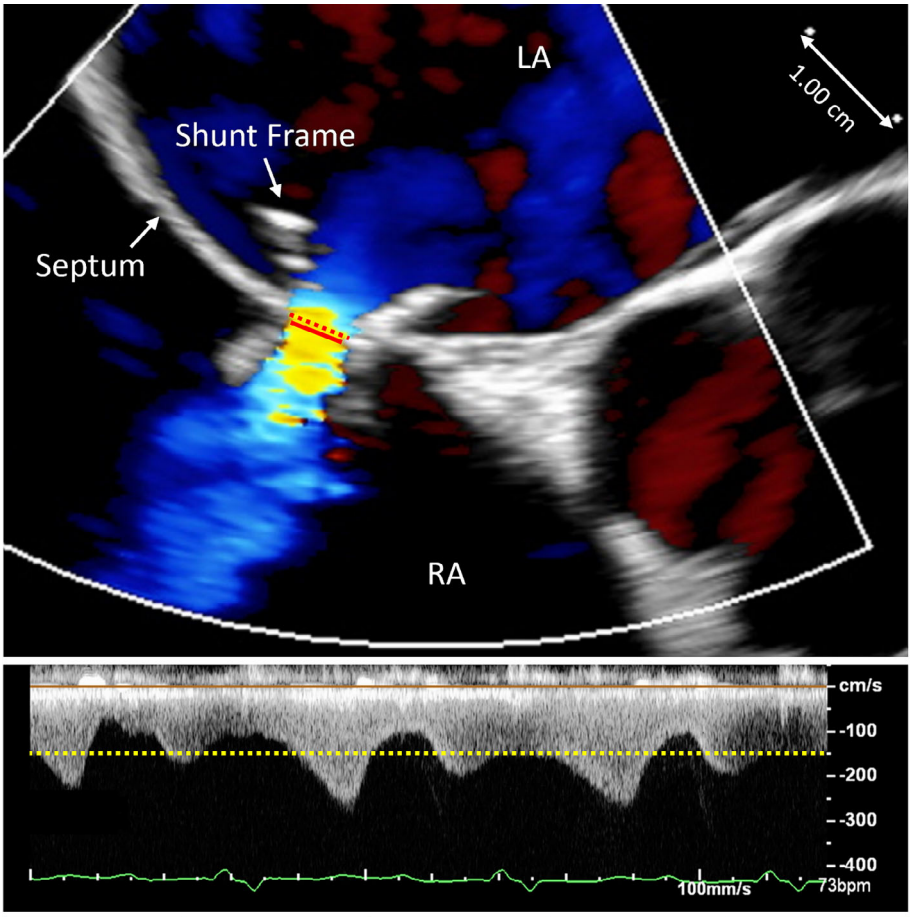

D_{vc}	D_{frame}	D_{eff}	$\Delta\overline{P}$	Q
0.46 cm	0.51 cm	0.47 cm	9.0 mmHg	1586 ml/min
Nominal Lumen (12 months)				

diameter of 0.47–0.48 cm predicted from CFD and bench flow studies. The likely cause is non-coplanar alignment of the echo beam with the long axis of the shunt. Using a simple first-order correction (Equation 4), the effective diameter D_{eff} at implant was 0.47 ± 0.01 cm, which closely matched theoretical simulations and bench measurements. Importantly, this adjustment significantly reduced shunt to shunt variance of orifice diameter seen with uncorrected measurements and helped to differentiate in-shunt stenosis from pseudo-stenosis. This type of first order correction is possible only when the shunt frame adjacent to the orifice can be visualized and accurately measured on the 2D echo portion of the same image containing the colour Doppler signal used to measure D_{vc} and because the true orifice diameter of the frame is reliably known.

There was a single instance of acquired shunt stenosis in a patient where the thickness of the interatrial septum exceeded the design limits established during pre-clinical animal trials. The present study, however, shows that when appropriately located the shunt is highly resistant to narrowing during the first year. This contrasts with an earlier version of the shunt which had a tri-leaflet tissue valve

Figure 4 Colour Doppler stenotic and pseudo stenotic shunt case examples. Top left: Short axis view of shunt with severely stenotic lumen at 6 month follow-up. Shunt is in the anterior septum and angulated towards the posterior wall of the aorta at lower right in location of foramen ovale. Top right: Short axis view of pseudo stenotic shunt lumen. Bottom: Table with measured values. ΔP^{-}, mean interatrial pressure gradient; D_{frame}, measured diameter of the frame neck; D_{eff}, effective diameter; D_{vc}, diameter *vena contracta*; Q, trans-shunt flow.

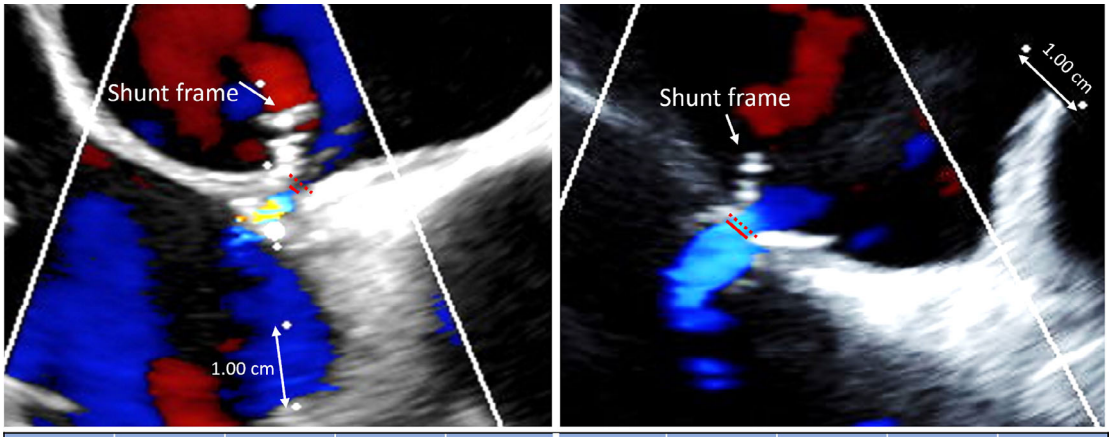

D_{vc}	D_{frame}	D_{eff}	$\Delta\bar{P}$	Q
0.09 cm	0.29 cm	0.16 cm	4.0 mmHg	125 ml/min
Stenotic Lumen (6 months)				

D_{vc}	D_{frame}	D_{eff}	$\Delta\bar{P}$	Q
0.33 cm	0.38 cm	0.44 cm	1.0 mmHg	470 ml/min
Pseudo-Stenotic Lumen (6 months)				

Figure 5 *In vivo* shunt orifice dimensions over time. Graphs showing individual patient transesophageal echocardiographic (TEE) measurements of *vena contracta*, frame neck, and effective diameters at implant and at 6 and 12 month follow-up. The stenotic threshold (red dashed line). Blue circles ● below this line indicate that the shunt orifice size was artifactually reduced due to non-coaxial imaging (pseudo stenotic). The red triangle ▲ represents a single patient with a stenotic shunt at 6 month follow-up. That patient exited the study upon receiving a left ventricular assist device (LVAD) at 8 months at which time the shunt was occluded. Mean ± standard deviation values are exclusive of stenotic shunt.

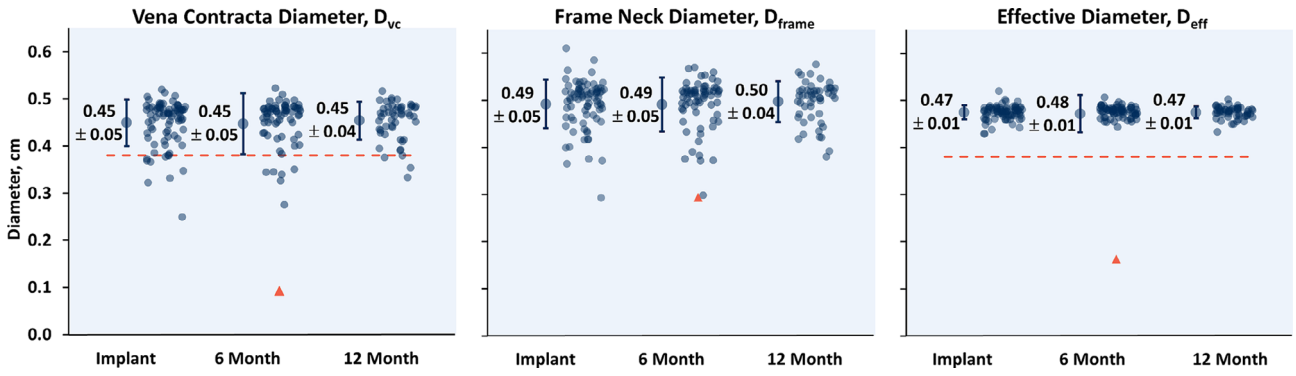

sutured to the right atrial side of the frame. That device had an ~50% rate of narrowing or occlusion by 12 months in humans, which was caused by pannus growth from the abluminal shunt surface extending into the valve commissures.[4]

Minimal late luminal loss observed in this study may be attributed to the combination of optimized shunt materials and geometry promoting more favourable host healing responses to vascular injury in the presence of foreign bodies. Clowes et al. demonstrated that less porous ePTFE vascular grafts, with internodal distance of 30 μ (like the shunt device) were eventually covered with neointima comprising fibroblasts, smooth muscles cells, and endothelium growing translationally from the adjacent artery along the lumen of the grafts.[23,24] It took up to 12 months to heal 6–9 cm long grafts in primates. When using ePTFE with 60 μ internodal

Figure 6 *In vivo* shunt flow/pressure relationship over time. Scatter plots showing transesophageal echocardiographic (TEE) measured shunt flow Q as a function of the mean interatrial pressure gradient ΔP^{-} at implant and at 6 month and 12 month follow-up. Top row: Q calculated using the *vena contracta* diameter (D_{vc}). Bottom row: Q calculated using the effective diameter (D_{eff}). Individual patient data ● (blue circles), with population means ± standard deviations (blue crosses with error bars). The red triangle ▲ represents a single patient with a stenotic shunt at 6 month follow-up. Patient data are compared with the model derived from computational fluid dynamics simulation (black curves).

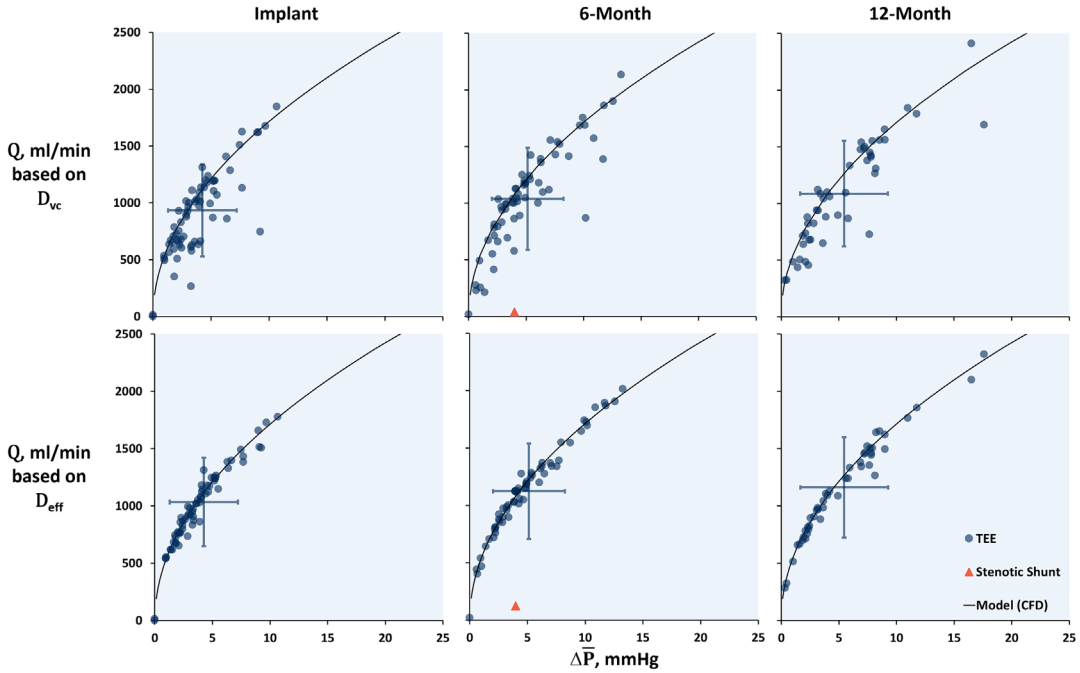

distance, capillaries derived from abluminal granulation tissue penetrated the graft matrix providing multiple sources for transmural smooth muscle cell migration, proliferation and extracellular matrix deposition on the luminal surface.[25] Thick pannus overgrowth during the first 6 to12 months has also been shown to interfere with the fidelity of a transeptally implanted left atrial pressure sensor in animals and humans.[26,27] Modifying the geometry of the device to position the sensing diaphragm several millimetres into the left atrium eliminated the problem. The shunt's encapsulated hourglass geometry establishes that the minimal distance for translational tissue growth required to reach the orifice exceeds 4 mm. Animal testing has confirmed that pannus growth is indeed translational, not transmural, and that the thickness of the neointima greatly diminishes prior to reaching the luminal surface of the shunt's orifice, which eventually is covered by a thin layer of neoendothelium.[4]

A key finding was that the shunt's flow versus pressure relationship measured by TEE closely matched fluid dynamics theory, validating this quantitative imaging modality for characterizing shunt performance both acutely and longer term. Expressing shunt patency simply as a binary (flow vs. no flow) parameter may be misleading since as in this study, a shunt was labelled patent even in the presence of severe, flow-limiting stenosis.

Lastly, the optimal interatrial shunt size for treating HF should strike a good balance between left ventricular unloading while avoiding right ventricular volume overload. The 0.51 cm orifice size shunt reliably yielded a Qp:Qs averaging 1.22. This orifice size in the earlier version of this shunt showed promise in a controlled ovine model of ischaemic cardiomyopathy, resulting in improvements in both left and right ventricular performance when the shunt remained patent.[28] Moreover, first in human experience with that shunt verified that when the *vena contracta* diameter was maintained, improvements in LV function and haemodynamics without deterioration of right ventricular function were observed at 12 month follow-up.[4] Thus, a small shunt with a durable orifice size may be beneficial and tolerated in HF patients who often have pre-existing right ventricular dysfunction.

Limitations

The limitations of two-dimensional TEE imaging for *vena contracta* assessment and acoustic artefacts from the metallic shunt frame may have affected the accuracy of some

measurements.[29–31] Three-dimensional TEE could potentially mitigate these limitations.[32,33] Also, the correction of using known frame geometry to compensate for TEE beam misalignment could yield spurious results if the shunt's lumen cross section were asymmetrically narrowed. Finally, we cannot exclude the possibility that there were alterations of the shunts in the patients who could not be assessed at follow-up. These limitations notwithstanding, the overall approach of using fluid dynamic theory and TEE imaging over 12 months provided robust insights for evaluating performance and physiology of this interatrial shunt device.

Conclusions

This study demonstrated concordance between CFD simulations, bench flow testing, and TEE measurements in patients with advanced HF implanted with the Ventura interatrial shunt. The shunt remained functional and widely patent with minimal late lumen loss after 1 year of follow-up, supporting its potential as a durable and well-balanced therapeutic option. Further clinical safety and effectiveness data from the RELIEVE-HF randomized cohort is expected in 2024 and may provide additional confirmation into the device's performance in HF patients.

Funding

We thank the V-Wave Ltd., Caesarea, Israel. The RELIEVE-HF Steering Committee designed the protocol with the study sponsor. All data collection, and data analysis was conducted by the Echocardiographic Core Laboratory at Penn State University and the Cardiovascular Research Foundation in NY, NY. The sponsor of the study contributed to the interpretation of the results.

Conflict of interest

Drs. Pfeiffer's, Boehmer's, and Gorcsan's employer, Penn State University, receives research fees from V-Wave supporting the RELIEVE-HF Echocardiography Core Laboratory. Dr. Pfeiffer has received speaker honoraria for Abbott and Ancora. Dr. Bayes has received speaker honoraria and/or consulting for AstraZeneca, Bayer, Boehringer Ingelheim, Novartis, Roche Diagnostics, Vifor. Dr Eigler is an employee and a shareholder of V-Wave. Dr. Abraham receives personal fees and is a shareholder of V-Wave. Dr. Stone has received speaker honoraria from Medtronic, Pulnovo, Infraredx, Abiomed, Amgen, Boehringer Ingelheim; has served as a consultant to Abbott, Daiichi Sankyo, Ablative Solutions, CorFlow, Cardiomech, Robocath, Miracor, Vectorious, Apollo Therapeutics, Valfix, TherOx, HeartFlow, Neovasc, Ancora, Elucid Bio, Occlutech, Impulse Dynamics, Adona Medical, Millennia Biopharma, Oxitope, Cardiac Success, HighLife; and has equity/options from Ancora, Cagent, Applied Therapeutics, Biostar family of funds, SpectraWave, Orchestra Biomed, Aria, Cardiac Success, Valfix, Xenter. Dr. Stone's employer, Mount Sinai Hospital, receives research grants from Abbott, Abiomed, Bioventrix, Cardiovascular Systems Inc, Phillips, Biosense-Webster, Shockwave, Vascular Dynamics, Pulnovo, V-wave. Dr. Núñez has received speaker honoraria and/or consulting for Alleviant, AstraZeneca, Bayer, Boehringer Ingelheim, Novartis, NovoNordisk, Rovi, and Vifor. Dr. Anker receives grants and personal fees from Vifor and Abbott Vascular, and personal fees for consultancies, trial committee work and/or lectures from Actimed, Amgen, Astra Zeneca, Bayer, Boehringer Ingelheim, Bioventrix, Brahms, Cardiac Dimensions, Cardior, Cordio, CVRx, Cytokinetics, Edwards, Farraday Pharmaceuticals, GSK, HeartKinetics, Impulse Dynamics, Novartis, Occlutech, Pfizer, Repairon, Sensible Medical, Servier, Vectorious, and V-Wave; is a named co-inventor of two patent applications regarding MR-proANP (DE 102007010834 & DE 102007022367), but he does not benefit personally from the related issued patents.

References

1. Shah SJ, Borlaug BA, Chung ES, Cutlip DE, Debonnaire P, Fail PS, *et al*. Atrial shunt device for heart failure with preserved and mildly reduced ejection fraction (REDUCE LAP-HF II): a randomised, multicentre, blinded, sham-controlled trial. *Lancet* 2022;**399**:1130-1140. doi:10.1016/S0140-6736(22)00016-2
2. Shah SJ, Feldman T, Ricciardi MJ, Kahwash R, Lilly S, Litwin S, *et al*. One-year safety and clinical outcomes of a transcatheter interatrial shunt device for the treatment of heart failure with preserved ejection fraction in the reduce elevated left atrial pressure in patients with heart failure (REDUCE LAP-HF I) trial: a randomized clinical trial. *JAMA Cardiol* 2018;**3**:968-977. doi:10.1001/jamacardio.2018.2936
3. Kaye DM, Hasenfuß G, Neuzil P, Post MC, Doughty R, Trochu JN, *et al*. One-year outcomes after transcatheter insertion of an interatrial shunt device for the management of heart failure with preserved ejection fraction. *Circ Heart Fail* 2016;**9**:e003662. doi:10.1161/CIRCHEARTFAILURE.116.003662
4. Rodés-Cabau J, Bernier M, Amat-Santos IJ, Ben Gal T, Nombela-Franco L, García del Blanco B, *et al*. Interatrial shunting for heart failure: early and late results from the first-in-human experience with the V-wave system. *JACC Cardiovasc Interv* 2018;**11**:2300-2310. doi:10.1016/j.jcin.2018.07.001
5. Paitazoglou C, Bergmann MW, Özdemir R, Pfister R, Bartunek J, Kilic T, *et al*. One-year results of the first-in-man study investigating the atrial flow regulator for left atrial shunting in symptomatic heart failure patients: the

PRELIEVE study. *Eur J Heart Fail* 2021;**23**:800-810. doi:10.1002/ejhf.2119
6. Sun W, Zou H, Yong Y, Liu B, Zhang H, Lu J, *et al*. The RAISE trial: a novel device and first-in-man trial. *Circ Heart Fail* 2022;**15**:e008362. doi:10.1161/CIRCHEARTFAILURE.121.008362
7. Barker CM, Meduri CU, Fail PS, Chambers JW, Solet DJ, Kriegel JM, *et al*. Feasibility of a no-implant approach to interatrial shunts: preclinical and early clinical studies. *Struct Heart* 2022;**6**:100078. doi:10.1016/j.shj.2022.100078
8. https://clinicaltrials.gov/ct2/show/NCT03499236.
9. Rodés-Cabau J, Lindenfeld J, Abraham WT, Zile MR, Kar S, Beyés-Genis A, *et al*. Interatrial shunt therapy in advanced heart failure: Outcomes from the open-label cohort of the RELIEVE-HF trial. *Eur J Heart Fail* 2024;38561314. doi:10.1002/ejhf.3215
10. Gorlin R, Gorlin SG. Hydraulic formula for calculation of the area of the stenotic mitral valve, other cardiac valves, and central circulatory shunts. *I Am Heart J* 1951;**41**:1-29. doi:10.1016/0002-8703(51)90002-6
11. Flachskampf FA, Weyman AE, Guerrero JL, Thomas JD. Influence of orifice geometry and flow rate on effective valve area: an in vitro study. *J Am Coll Cardiol* 1990;**15**:1173-1180. doi:10.1016/0735-1097(90)90260-V
12. Pocock SJ, Ariti CA, McMurray JJ, Maggioni A, Køber L, Squire IB, *et al*. Predicting survival in heart failure: a risk score based on 39,372 patients from 30 studies. *Eur Heart J* 2013;**34**:1404-1413. doi:10.1093/eurheartj/ehs337
13. Lupón J, de Antonio M, Vila J, Peñafiel J, Galán A, Zamora E, *et al*. Development of a novel heart failure risk tool: the Barcelona bio-heart failure risk calculator (BCN bio-HF calculator). *PLoS ONE* 2014;**9**:e85466. doi:10.1371/journal.pone.0085466
14. Morris PD, Narracott A, von Tengg-Kobligk H, Silva Soto DA, Hsiao S, Lungu A, *et al*. Computational fluid dynamics modelling in cardiovascular medicine. *Heart* 2016;**102**:18-28. doi:10.1136/heartjnl-2015-308044
15. Hollingshead CL, Johnson MC, Barfuss SL, Spall R. Discharge coefficient performance of Venturi, standard concentric orifice plate, V-cone and wedge flow meters at low Reynolds numbers. *J Petrol Sci Eng* 2011;**78**:559-566. doi:10.1016/j.petrol.2011.08.008
16. Nevaril CG, Lynch EC, Alfrey CP Jr, Hellums JD. Erythrocyte damage and destruction induced by shearing stress. *J Lab Clin Med* 1968;**71**:784-790.
17. Kameneva MV, Burgreen GW, Kono K, Repko B, Antaki JF, Umezu M. Effects of turbulent stresses upon mechanical hemolysis: experimental and computational analysis. *ASAIO J* 2004;**50**:418-423. doi:10.1097/01.MAT.0000136512.36370.B5
18. Leverett LB, Hellums JD, Alfrey CP, Lynch EC. Red blood cell damage by shear stress. *Biophys J* 1972;**12**:257-273. doi:10.1016/S0006-3495(72)86085-5
19. Ahmed M, Gupta N, Jana R, Das MK, Kar KK. Ramifications of vorticity on aggregation and activation of platelets in bi-leaflet mechanical heart valve: fluid–structure-interaction study. *J Biomech Eng* 2022;**144**:081002. doi:10.1115/1.4053665
20. Stein P, Sabbah HN. Turbulent blood flow in the ascending aorta of humans with normal and diseased aortic valves. *Circ Res* 1976;**39**:58-65. doi:10.1161/01.RES.39.1.58
21. Kozłowski M, Wojtas K, Orciuch W, Jędrzejek M, Smolka G, Wojakowski W, *et al*. Potential applications of computational fluid dynamics for predicting hemolysis in mitral paravalvular leaks. *J Clin Med* 2021;**10**:5752. doi:10.3390/jcm10245752
22. Fraser KH, Zhang T, Taskin ME, Griffith BP, Wu ZJ. A quantitative comparison of mechanical blood damage parameters in rotary ventricular assist devices: shear stress, exposure time and hemolysis index. *J Biomech Eng* 2012;**134**:081002. doi:10.1115/1.4007092
23. Clowes AW, Kirkman TR, Reidy MA. Mechanisms of arterial graft healing. Rapid transmural capillary ingrowth provides a source of intimal endothelium and smooth muscle in porous PTFE prostheses. *Am J Pathol* 1986;**123**:220-230.
24. Clowes AW, Kirkman TR, Clowes MM. Mechanisms of arterial graft failure. II. Chronic endothelial and smooth muscle cell proliferation in healing polytetrafluoroethylene prostheses. *J Vasc Surg* 1986;**3**:877-884. doi:10.1016/0741-5214(86)90154-0
25. Clowes AW, Gown AM, Hanson SR, Reidy MA. Mechanisms of arterial graft failure. 1. Role of cellular proliferation in early healing of PTFE prostheses. *Am J Pathol* 1985;**118**:43-54.
26. Trainor KE, Roberts A, Weeks B, Jackson N, Troughton RW, Charles CJ, *et al*. Comparative pathology of an implantable left atrial pressure sensor. *ASAIO J* 2013;**59**:486-492. doi:10.1097/MAT.0b013e31829bdffd
27. The HOMEOSTASIS Investigators, Troughton RW, Ritzema J, Eigler NL, Melton IC, Krum H, *et al*. Direct left atrial pressure monitoring in severe heart failure: long-term sensor performance. *J Cardiovasc Transl Res* 2011;**4**:3-13. doi:10.1007/s12265-010-9229-z
28. Eigler NL, del Rio CL, Verheye S, McConnell PI, Lilly SM, George R, *et al*. Cardiac unloading with an implantable interatrial shunt in heart failure: serial observations in an ovine model of ischemic cardiomyopathy. *Struct Heart* 2017;**1**:40-48. doi:10.1080/24748706.2017.1326647
29. Hall SA, Brickner ME, Willett DL, Irani WN, Afridi I, Grayburn PA. Assessment of mitral regurgitation severity by Doppler color flow mapping of the vena contracta. *Circulation* 1997;**95**:636-642. doi:10.1161/01.CIR.95.3.636
30. Zoghbi WA, Adams D, Bonow RO, Enriquez-Sarano M, Foster E, Grayburn PA, *et al*. Recommendations for noninvasive evaluation of native valvular regurgitation: a report from the American Society of Echocardiography developed in collaboration with the Society for Cardiovascular Magnetic Resonance. *J Am Soc Echocardiogr* 2017;**30**:303-371. doi:10.1016/j.echo.2017.01.007
31. Biner S, Rafique A, Rafii F, Tolstrup K, Noorani O, Shiota T, *et al*. Reproducibility of proximal isovelocity surface area, vena contracta, and regurgitant jet area for assessment of mitral regurgitation severity. *JACC Cardiovasc Imaging* 2010;**3**:235-243. doi:10.1016/j.jcmg.2009.09.029
32. Yosefy C, Hung J, Chua S, Vaturi M, Ton-Nu TT, Handschumacher MD, *et al*. Direct measurement of vena contracta area by real-time 3-dimensional echocardiography for assessing severity of mitral regurgitation. *Am J Cardiol* 2009;**104**:978-983. doi:10.1016/j.amjcard.2009.05.043
33. Zeng X, Levine RA, Hua L, Morris EL, Kang Y, Flaherty M, *et al*. Diagnostic value of vena contracta area in the quantification of mitral regurgitation severity by color Doppler 3D echocardiography. *Circ Cardiovasc Imaging* 2011;**4**:506-513. doi:10.1161/CIRCIMAGING.110.961649